FT-EPR Study of Photoinduced Electron Transfer at the Surface of TiO_2 Nanoparticles

Débora M. Martino,† Hans van Willigen,* and Mark T. Spitler

Department of Chemistry, University of Massachusetts at Boston, Boston, Massachusetts 02125

Received: May 20, 1997; In Final Form: August 1, 1997[⊗]

Photoinduced electron transfer at the surface of TiO_2 nanoparticles in ethanol has been studied with Fourier transform EPR (FT-EPR). Measurements were performed on three systems: (1) a solution of coumarin 343 (C343) dye and methyl viologen (MV^{2+}) in ethanol, (2) a colloidal solution of TiO_2 in ethanol containing MV^{2+}, and (3) a colloidal solution of TiO_2 in ethanol containing both C343 and MV^{2+}. In the C343/MV^{2+} system, pulsed-laser (355 nm) excitation of the dye results in MV^{2+} reduction. The rate constant of the photoinduced electron-transfer reaction, derived from the time profile of the FT-EPR spectrum of the MV^+ radical, was found to be $\sim 5 \times 10^9$ M^{-1} s^{-1}, consistent with a near diffusion controlled reaction. Bandgap excitation (308 nm) of the semiconductor particles in the TiO_2/MV^{2+} system also gives rise to MV^+ formation. In this case the FT-EPR signal growth can be described by a single exponential with rate constant $k_f = 0.41 \times 10^6$ s^{-1}. The kinetics indicates that MV^{2+} reduction involves photogenerated electrons trapped on the TiO_2 particles and is controlled by interfacial charge transfer rather than diffusive encounters of acceptor molecules with TiO_2 particles. Dye-sensitized formation of MV^+ radicals is observed as well following laser (355 nm) excitation of the C343/MV^{2+}/TiO_2 system. However, whereas the MV^+ spectrum produced by the C343/MV^{2+} system reaches its maximum intensity around 100 ns after laser excitation, in the presence of TiO_2 the maximum is found tens of microseconds after the laser pulse. The time profile of MV^+ formation in this case follows first-order kinetics with a time dependent rate constant, $k_f = k_0 t^{\alpha-1}$, where both k_0 and α are a function of the degree of dye adsorption onto the TiO_2 particles and the pH of the solution. In this system, the trapped electrons responsible for MV^{2+} reduction are generated by excitation of adsorbed dye molecules, which leads to electron injection into the conduction band of the semiconductor. Dye-sensitization of the TiO_2 particles strongly increases the free radical yield. However, as the surface coverage by dye molecules approaches saturation level, the rate of electron transfer from semiconductor particles to acceptor molecules in solution is strongly attenuated.

I. Introduction

Photoinduced electron-transfer reactions catalyzed by semiconductor particles are of considerable interest because of applications in chemical synthesis,[1] solar energy conversion,[2] and decomposition of organic pollutants.[3] Upon bandgap excitation, charge carriers can initiate oxidation and reduction of molecules adsorbed on the semiconductor particles. Since this redox chemistry gives rise to paramagnetic species, electron paramagnetic resonance (EPR) can be a valuable source of information on reaction mechanisms and dynamics. This is illustrated, for instance, by continuous wave (CW) EPR studies of charge carrier trapping sites in TiO_2 at cryogenic temperatures[4−7] and studies of the formation of transient free radicals in liquid solution by bandgap irradiation of semiconductor suspensions using the spin-trapping technique.[8,9] In a few cases, the EPR spectra of short-lived paramagnetic species in liquid solution, formed by continuous irradiation of semiconductor suspensions, also have been detected directly.[10,11]

So far applications of EPR all have dealt with photostationary states and, therefore, provide no direct information on the dynamics of interfacial redox chemistry. Here we report on the application of Fourier transform EPR[12] (FT-EPR) in time-resolved measurements of free radicals formed by pulsed-laser excitation of colloidal TiO_2 solutions. It is shown that with FT-EPR the time course of electron transfer across the particle−solution interface can be monitored. High spectral resolution makes it possible to identify free radicals formed and to draw conclusions regarding their location in the microheterogeneous medium.

Of special interest in this investigation was the *large bandgap semiconductor* TiO_2 of which the photoresponse was extended into the visible region of the spectrum by adsorption of coumarin 343 (C343) dye molecules. In this system, excitation of the adsorbed dye molecules results in electron injection into the conduction band.[13] Photoelectrochemical experiments have shown that C343 displays a high efficiency in the spectral sensitization of semiconductors.[13] This has been observed as well with dyes such as eosin,[14] tris(4,4′-dicarboxy-2,2′-bipyridine)ruthenium[15] and [tetrakis(4-carboxylphenyl)porphyrinato]-zinc (ZnTPPC)[16] and is attributed to the presence of carboxylic groups, which can give rise to strong surface bonding and may facilitate electron transfer across the particle−solution interface.[17] The reported incident photon to current conversion efficiency for the TiO_2/C343 system exceeds 80% in the region of the absorption maximum of the dye (440 nm) and exceeds 70% for the wavelength range between 400 and 500 nm.[13] Our study focused on the reduction of the methyl viologen dication (MV^{2+}) by electron transfer from TiO_2 nanoparticles and compares the course of the reaction initiated by direct bandgap excitation with the dye-sensitized electron-transfer process. The measurements provide information on the kinetics of electron transfer to MV^{2+} following electron injection in the TiO_2 conduction band.

* To whom the correspondence should be addressed.
† On leave from the Physics Department, FBCB, UNL, 3000 Santa Fe, Argentina.
⊗ Abstract published in *Advance ACS Abstracts,* October 1, 1997.

S1089-5647(97)01682-9 CCC: $14.00

II. Experimental Section

The bipyridinium dication salt 1,1′-dimethyl-4,4′-bipyridinium dichloride (MV^{2+}, **I**), coumarin 343 (C343, **II**), and the TEMPONE (d_{16}) nitroxide spin label were obtained from Aldrich and used as received. Ethanol (anhydrous, Pharmco) was used without further purification. TiO_2 colloidal solutions in ethanol were prepared from titanium isopropoxide (Aldrich) following the procedure described elsewhere.[18] The hydrolysis was carried out in the presence of 3% acetic acid, and a transparent solution with final Ti^{4+} concentration of 0.02 M and pH between 3.5 and 3.8 was obtained. The average size of the particles has been reported to be around 50-60 Å.[18] Absorption spectra of the colloidal solutions showed no significant light absorption above 330 nm.

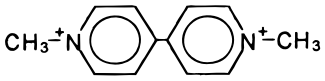

Methylviologen , I

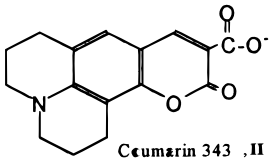

Coumarin 343 , II

Measurements were performed on ethanol solutions containing C343 (9×10^{-5} to 7×10^{-4} M) and MV^{2+} (1×10^{-3} to 4×10^{-3} M), on TiO_2 colloidal solutions with MV^{2+} (1×10^{-3} M) and on TiO_2 colloidal solutions with C343 (9×10^{-5} to 7×10^{-4} M) and MV^{2+} (1×10^{-3} to 4×10^{-3} M).

UV/vis absorption and fluorescence spectra were recorded with a Uvikon 860 (Kontron Instruments) spectrometer and a Perkin-Elmer LS-5B spectrometer, respectively.

FT-EPR measurements were performed with a home-built spectrometer.[19,20] The response of the sample to the $\pi/2$ microwave pulse was detected in quadrature with application of a CYCLOPS phase-cycling routine. The sample solution was deoxygenated by sparging with nitrogen gas prior to and during measurements and pumped through a quartz EPR flow cell held in the microwave cavity. Solutions containing the C343 dye were excited with the third harmonic (355 nm) of a Quanta Ray GCR12 Nd:YAG laser (pulse width 8 ns, pulse energy ~20 mJ, pulse repetition rate 10 Hz), while solutions without dye were excited with 308 nm light from a Lambda Physik (EMG103) XeCl excimer laser (pulse energy ~25 mJ, pulse repetition rate 10 Hz). All measurements were performed at room temperature. The free induction decay (FID) produced by a $\pi/2$ (15 ns) microwave pulse was recorded for a series of delay times (10 ns $< \tau_d <$ 1 ms) between laser excitation and microwave pulse. In most experiments, the FID was the time average of signals generated by a total of 400 laser shots (100 per phase). The amplitudes, phases, and line widths of resonance peaks were derived from the FIDs with a LPSVD analysis routine.[21] The spectrum of MV^+ covers a frequency range that exceeds the bandwidth of the spectrometer; thus the EPR spectra presented in the figures are assembled from signals obtained with three field settings.

The spin−lattice relaxation time (T_1) of MV^+ in methanol, prepared by chemical reduction of MV^{2+}, was measured with the inversion recovery method. A $\pi - \tau - (\pi/2 - \tau_{fix} - \pi - \tau_{fix})$ microwave pulse sequence was used in which the spin−echo was recorded for settings ranging from 270 ns to 200 μs. T_1 was calculated from a least-squares fit of the dependence of the integrated echo signal ($S(\tau)$) to the equation

$$S(\tau) = S(\tau \rightarrow \infty) - [S(\tau \rightarrow \infty) - S(\tau = 0)] \exp(-T_1^{-1}\tau)$$

III. Results and Discussion

a. C343/MV^{2+} in Ethanol. Figure 1a shows the FT-EPR spectrum of MV^+ produced by excitation (355 nm) of a deaerated ethanol solution containing C343 (7×10^{-4} M) and MV^{2+} (1×10^{-3} M). The hyperfine pattern can be simulated (cf. bottom of Figure 1) with the hyperfine splitting constants 1.35 (4H), 1.60 (4H), 4.06 (6H), and 4.22 G (2N). These values are in good agreement with literature values for the MV^+ radical (1.343 (4H), 1.591 (4H), 4.012 (6H), and 4.247 G (2N)).[22] It was verified that irradiation of a solution of MV^{2+} alone in ethanol does not lead to radical formation.

The formation of MV^+ upon irradiation of the C343/MV^{2+} sample can be attributed to oxidative quenching of C343 triplets formed by intersystem crossing (isc) from the excited singlet state. The sequence of events triggered by laser excitation of the dye molecules is given by

$$C343(S_0) \xrightarrow{h\nu} C343(S_1) \xrightarrow{\text{isc}} C343(T_1)$$

$$C343(T_1) + MV^{2+} \xrightarrow{k_{et}} C343^+ + MV^+ \qquad (1)$$

where k_{et} is the electron-transfer rate constant. Irradiation leads to a gradual change in color of the sample; this shows that the electron-transfer reaction is not completely reversible and is in competition with radical scavenging reactions. The cation radical $C343^+$ generated in the electron-transfer process could not be detected with FT-EPR; this is attributed to a short T_2. In contrast, we found that *in situ* electrochemical oxidation of C343 in acetonitrile produces a free radical that gives rise to a broad-line (CW) EPR spectrum with partially resolved hyperfine structure and covering a 100 G field range. This signal decays within 3−5 min upon interruption of the electrolysis.

The spectrum of MV^+ is entirely in absorption at all delay time settings. By performing FT-EPR measurements on C343/MV^{2+} in the presence of the TEMPONE(d_{16}) nitroxide radical (1.8×10^{-3} M), it was established that the electron-transfer process generates chemically induced dynamic electron polarization (CIDEP). Pulsed-laser excitation of this sample produces a transient increase in intensity of the nitroxide resonance peaks due to electron spin polarization transfer from MV^+ radicals. Figure 2 illustrates this effect for the center peak in the TEMPONE spectrum for a delay of 0.21 μs between laser excitation and microwave pulse where the signal enhancement amounts to 60% of the steady-state signal intensity. The effect shows that electron transfer from C343 triplets to MV^{2+} produces free radicals with excess population of the β electron spin state. The net absorptive polarization is attributed to spin polarization carried over from the C343 triplets (triplet mechanism CIDEP[23]). It is estimated that because of this CIDEP mechanism, the MV^+ signal intensity is ~10 times stronger than what would have been observed under thermal equilibrium conditions.

The time evolution of the intensity of the MV^+ spectrum was measured by varying the delay time τ_d between laser and microwave pulses and is depicted in Figure 3. The solid line in Figure 3 represents the least-squares fit of the data to the equation that applies if signal growth and decay are first-order processes. The signal grows in with rate constant $k_{et} \sim 6 \times 10^6$ s^{-1}, which is consistent with a diffusion-controlled electron-transfer reaction ($[MV^{2+}] = 1 \times 10^{-3}$ M). The rate of decay of the MV^+ signal is $\sim 5 \times 10^6$ s^{-1}. An independent measurement of the spin−lattice relaxation time of MV^+ using

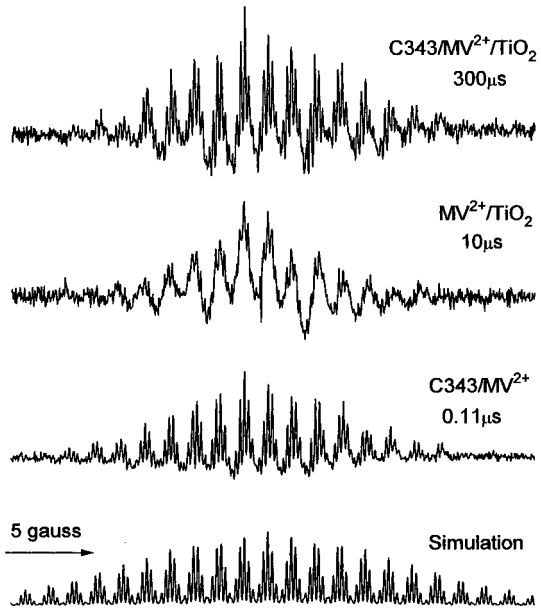

Figure 1. FT-EPR spectra of MV^+ produced by excitation of deaerated solutions containing (a) C343 (7×10^{-4} M) and MV^{2+} (1×10^{-3} M) in ethanol, (b) MV^{2+} (1×10^{-3} M) in TiO_2, and (c) C343 (7×10^{-4} M)/MV^{2+} (1×10^{-3} M) in TiO_2. The delay (τ_d) between laser and microwave pulses is given in the spectra. The simulated spectrum of MV^+ is given at the bottom of the figure.

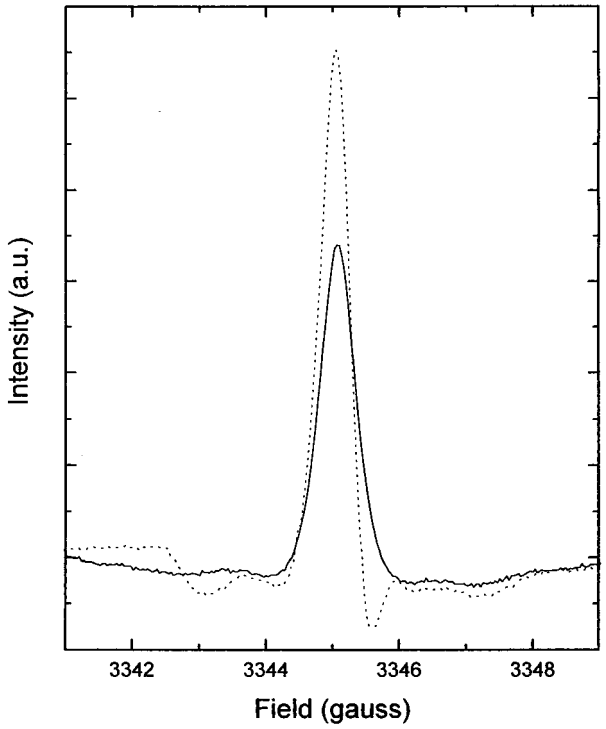

Figure 2. Center line of the FT-EPR spectrum of TEMPONE(d_{16}) (1.8×10^{-3} M) in a deaerated ethanol solution containing C343 (7×10^{-4} M) and MV^{2+} (1×10^{-3} M) before (solid line) and after (τ_d = 0.21 μs, dotted line) excitation.

the inversion recovery method gives $T_1 = 5.7\ \mu$s. This indicates that signal decay is determined mainly by back electron transfer and/or radical scavenging reactions and that relaxation of the spin system to thermal equilibrium makes only a minor contribution.

b. MV^{2+}/TiO_2 in Ethanol. Bandgap excitation (308 nm) of colloidal TiO_2 particles in ethanol containing methyl viologen (1×10^{-3} M) also generates MV^+ (cf. Figure 1b). It is evident from the time profile of the MV^+ signal intensity shown in

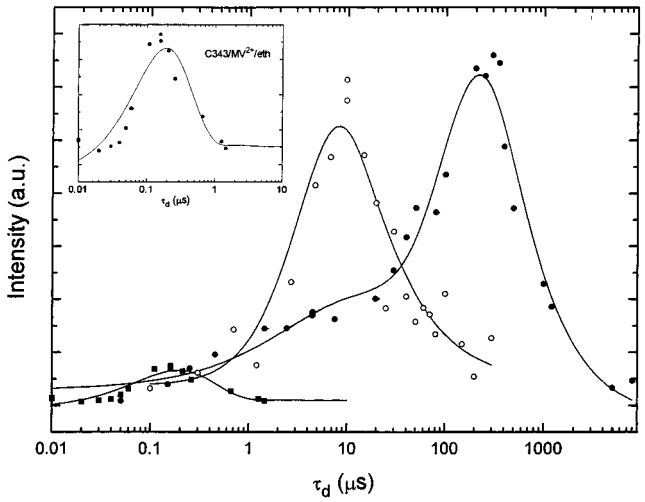

Figure 3. Time profiles of MV^+ signal intensities given by (■) C343 (7×10^{-4} M)/MV^{2+} (1×10^{-3} M)/ethanol, (○) MV^{2+} (1×10^{-3} M)/TiO_2, and (●) C343 (7×10^{-4} M)/MV^{2+} (1×10^{-3} M)/TiO_2. Solid lines represent least-squares fits of the data assuming first-order kinetics of formation and decay

Figure 3 that reduction mediated by photoexcitation of colloidal TiO_2 introduces striking changes both in the intensity of the spectrum and in rates of signal growth and decay compared to that found for C343/MV^{2+} in ethanol. In this case it can be concluded that the spin system is at thermal equilibrium because signal decay ($k_d = 0.5 \times 10^5\ s^{-1}$) is slow compared to the measured spin−lattice relaxation rate of $1.8 \times 10^5\ s^{-1}$ (see above). A comparison of integrated signal intensities obtained with C343/MV^{2+} (100 ns) and MV^{2+}/TiO_2 (10 μs) shows an increase by a factor of 4. Since spin polarization enhances the signal intensity in the former system by about a factor of 10, the yield of free radicals increases by at least an order of magnitude upon going to the MV^{2+}/TiO_2 system. At the same time the rate of formation is reduced to $0.41 \times 10^6\ s^{-1}$ and the maximum signal intensity is observed at about 10 μs, whereas it was around 100 ns in homogeneous solution. Flash photolysis studies of MV^{2+} reduction by photoexcitation of TiO_2 nanoparticles in water[24] and acetonitrile[25] also revealed a relatively slow electron-transfer process occurring over a time period of tens of microseconds.

The kinetics indicates that the interfacial electron-transfer reaction involves photogenerated electrons trapped within the TiO_2 bandgap (also called "subbandgap states"[26]). Formation of long-lived trapped electrons ($e_{trap}^{TiO_2}$) upon UV irradiation of colloidal TiO_2 solutions in ethanol has been reported earlier by Kamat et al.[18] and was found as well for TiO_2 suspensions in aqueous solution.[24,26] In agreement with results reported by Kamat et al.[18] we found that deaerated TiO_2 colloidal solutions turn blue upon exposure to UV light. That the color change arises as a result of trapping of photogenerated charge carriers within the semiconductor nanocrystals is confirmed by our finding that addition of MV^{2+} *subsequent* to irradiation leads to MV^+ formation.

The relatively slow rate of MV^+ formation can be attributed to a combination of two factors. First, if the energetics of these interfacial electron transfers in ethanol are similar to that in aqueous solution, the thermodynamic driving force will be small. For TiO_2 particles in water, the potential at the conduction band edge is given by $E_{CB} = -0.1 - 0.059 \times (\text{pH})$ V.[27] With a pH independent MV^{2+} reduction potential, $E°(MV^{2+}/MV^+) = -0.448$ V (vs NHE in water),[24] the electron transfer is predicted to be an endothermic process in acidic solutions. Indeed, flash photolysis measurements have shown that the rate constant of

MV^{2+} reduction in irradiated aqueous TiO_2 solution is $\sim 3 \times 10^6$ M^{-1} s^{-1} at pH 4 and increases markedly with increasing pH as a result of the shift in E_{CB} value.[24] The second factor is the geometric constraint imposed on the electron-transfer process; that is, only a fraction of encounters of acceptors with nanoparticles will bring $e_{trap}^{TiO_2}$ and MV^{2+} within electron-transfer range.

In the case of MV^{2+}/TiO_2, the electron-transfer reaction is not reversible and MV^+ signal decay ($k_d = 0.5 \times 10^5$ s^{-1}) is attributed to radical scavenging reactions.

c. C343/MV^{2+}/TiO_2 in Ethanol. FT-EPR spectra of MV^+ generated by laser excitation (355 nm) of a deaerated solution containing C343 (7×10^{-4} M)/MV^{2+} (1×10^{-3} M) and TiO_2 (cf. Figures 1c and 3) show that the addition of TiO_2 modifies the mechanism of electron transfer from C343 to MV^{2+}. In the presence of the semiconductor particles the MV^+ signal intensity increases by a factor of 6 compared to that found for homogeneous solution and the electron-transfer process does not lead to rapid sample degradation, contrary to what is found for the C343/MV^{2+} and MV^{2+}/TiO_2 solutions.

Previous optical studies have shown that photoexcitation of C343 adsorbed on TiO_2 particles leads to electron injection with a quantum yield close to unity[13,28] from the singlet excited state of the dye into the semiconductor conduction band. In the present system, dye adsorption and electron injection are confirmed by data from optical spectroscopy. The absorption spectrum of C343 (2×10^{-5} M) in TiO_2 colloidal solution exhibits a $\sim$10 nm red shift, without significant change in band shape, compared with that of an ethanol solution of the dye. The shift is attributed to the interaction between the TiO_2 particle and the dye molecule. From the optical data it can be deduced that dye adsorption must be nearly quantitative. Similar shifts were observed in the absorption spectrum of eosin Y upon adsorption on the surface of colloidal TiO_2 particles[14] and on ZnO powder.[29] Electron-transfer quenching of the singlet excited state of C343 in TiO_2 solutions is evident from the $\sim$70% decline in fluorescence compared with that in ethanol. From the earlier transient optical absorption studies[13,28] combined with the present optical absorption and fluorescence data it can be concluded that photoexcitation of the dye molecules in the C343/MV^{2+}/TiO_2 system leads to electron transfer to the semiconductor conduction band, which is followed by interfacial electron transfer to MV^{2+} in solution.

Growth and decay of signal intensities have been fit to the equation that applies if radical formation and decay are first-order processes. As shown in Figure 3, the time profile of MV^+ formation in the C343 (7×10^{-4} M)/MV^{2+} (1×10^{-3} M)/TiO_2 system can be described satisfactorily with first-order kinetics with time dependent rate constant $k_f = k_0 t^{\alpha-1}$, where $k_0 = 0.033 \times 10^6$ s^{-1} and $\alpha = 0.81$. Since charge injection from the singlet excited state into the TiO_2 conduction band occurs in the picosecond time domain ($k_{inj} \approx 5 \times 10^{12}$ s^{-1}),[28] it is clear that this process does not affect the kinetics of MV^+ formation. It has also been found that, in the absence of conduction band electron ($e_{CB}^{TiO_2}$) or hole ($C343^+$) scavenging, electron−hole recombination is a relatively fast process occurring in the nanosecond to microsecond time domain.[14] The time profile, therefore, points to a reduction step involving trapped electrons in which the reaction kinetics is governed by interfacial electron transfer from surface trapping sites to acceptor molecules. The overall reaction scheme can be summarized as follows:

$$C343(S_0) \xrightarrow{h\nu} C343(S_1)$$

$$C343(S_1) \xrightarrow{k_{inj}} C343^+ + e_{CB}^{TiO_2} \quad (2)$$

$$C343^+ + e_{CB}^{TiO_2} \xrightarrow{k_{bet}} C343(S_0) \quad (3)$$

$$e_{CB}^{TiO_2} \xrightarrow{k_{tr}} e_{trap}^{TiO_2} \quad (4)$$

$$MV^{2+} + e_{trap}^{TiO_2} \xrightarrow{k_f = k_0 t^{\alpha-1}} MV^+ \quad (5)$$

$$C343^+ + e_{trap}^{TiO_2} \xrightarrow{k_d} C343(S_0) \quad (6)$$

where k_{inj} is the rate of electron injection from the C343(S1) state into the TiO_2 particle and k_{bet} is the back electron-transfer rate. Back electron transfer (3) is a fast process and competes with $e_{trap}^{TiO_2}$ formation and eventual MV^{2+} reduction. Under the conditions of the measurements, it is likely that only a fraction of injected electrons are involved in MV^+ formation because of back electron-transfer processes (3) and (6). The generation of trapped electrons upon photoinduced electron injection into colloidal semiconductors is supported by results of a flash photolysis study by Moser and Grätzel.[14] These authors found that back electron transfer from TiO_2 to adsorbed dye molecules occurs in part via a fast process with a rate constant of 2×10^5 s^{-1} and in part via a slower process with a time constant ($\sim$230 μs) similar to that found in our measurements.

A pronounced change in the time profile of the signal intensity of the MV^+ spectrum was observed for the C343/MV^{2+}/TiO_2 system upon a reduction in dye concentration. Figure 4 illustrates the effect of an 8-fold reduction in dye concentration. It is apparent that *the rate of MV^+ formation increases as the C343 concentration is reduced*. The rate increase is accompanied by a significant increment in yield of MV^+. By contrast, a change in acceptor concentration (from 1×10^{-3} to 4×10^{-3} M) has no noticeable effect on rate of radical formation and yield. These results establish that interfacial electron transfer indeed controls the kinetics of radical formation. Moreover, they show that the degree of TiO_2 particles surface coverage by dye molecules affects the rate of electron capture by MV^{2+}. At a concentration of 7×10^{-4} M, dye adsorption amounts to about 70 molecules/particle which with $\sim$100 Å^2/molecule is close to the saturation level. At this coverage, dye molecules can be expected to inhibit reactive encounters of MV^{2+} molecules with TiO_2 particles. As a result, the rate of reduction (k_f) decreases and a larger fraction of trapped electrons recombine with dye cations. With [C343] = 9×10^{-5} M, trapped electrons at surface sites become more accessible, increasing the rate of formation and yield of MV^+. The dye coverage effect on reaction 5 also accounts for the pronounced decrease in rate of MV^+ formation going from MV^{2+}/TiO_2 to C343/MV^{2+}/TiO_2.

With [C343] = 7×10^{-4} M, the time profile of radical formation and decay also shows a remarkable aging effect. Figure 5 displays the time profiles for a sample measured immediately following addition of acceptor and dye to a colloidal solution of TiO_2 ($[MV^+]_{max}$ at $\sim$300 μs) and after a 3-day aging period ($[MV^+]_{max}$ at $\sim$40 μs).[30] Accompanying the changes in kinetics is a growth in signal intensity of more than a factor of 2. The aging period also affects dye fluorescence (cf. inset Figure 5) and the pH of the solution. Fluorescence quenching increases from 70% immediately after sample preparation to 86% after aging. The fluorescence intensity of C343 in ethanol remains unchanged over the same time period. The effect of dye concentration on the rate of MV^{2+} reduction

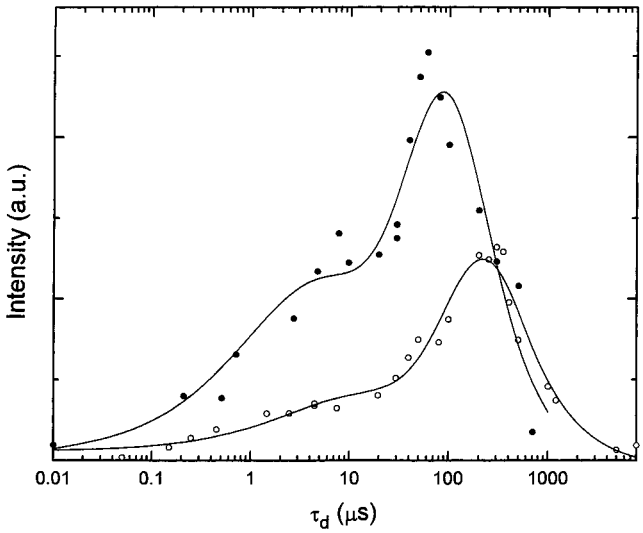

Figure 4. Time profiles of MV^+ signal intensities for (○) C343 (7×10^{-4} M)/MV^{2+} (1×10^{-3} M)/TiO_2 and (●) C343 (9×10^{-5} M)/MV^{2+} (1×10^{-3} M)/TiO_2. Solid lines represent least-squares fits of the data assuming first-order radical formation and decay kinetics, with a time dependent rate constant of formation (see text). The intensity scale is linear.

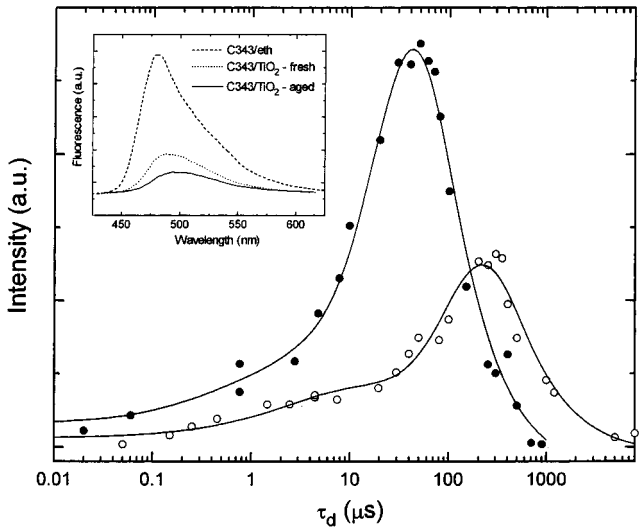

Figure 5. Time profiles of MV^+ signal intensities for C343 (7×10^{-4} M)/MV^{2+} (1×10^{-3} M)/TiO_2 measured immediately after preparation (○) and after a 3-day aging period (●). Solid lines represent least-squares fits of the data assuming first-order formation and decay kinetics, with a time dependent rate constant of formation (see text). The inset shows the fluorescence spectrum of C343 in ethanol, and in fresh and aged colloidal TiO_2 solutions. The intensity scale is linear.

shown in Figure 4 establishes that the marked rise in electron-transfer rate constant associated with the aging process cannot be due to increased dye adsorption. Instead, the increase in k_f may be due to the increase in pH from 4.8 to 5.8 over the 3-day period. The pH increase, on the one hand, is expected to increase the thermodynamic driving force of the electron-transfer process and, on the other hand, will reduce the Coulombic repulsion between the TiO_2 particles (which will be less positively charged at higher pH) and MV^{2+}. With a reduction in repulsion, MV^{2+} can remain longer at and closer to the particle surface, increasing the probability of electron transfer. The aging effects, in part, may stem as well from a gradual process by which dye molecules find optimum binding sites at the particle surface. This may account for the increase in fluorescence quenching. Changes in dye binding, which involves the carboxyl group, also can account for the pH change. At lower dye concentration (9×10^{-5} M) no significant aging effect was found.

As noted above, the time profile of MV^+ formation does not fit an exponential with time independent rate constant, but instead can be described with a stretched exponential in which the rate constant is given by $k_f = k_0 t^{\alpha-1}$. This function has been used to model the kinetics of photochemical reactions in heterogeneous media where there is a distribution in the value of first-order reaction rates.[31] With [C343] $= 7 \times 10^{-4}$ M, the distribution of rate constants gets narrower upon aging of the solution; from $k_0 = 0.033 \times 10^6$ s^{-1} and $\alpha = 0.81$ to $k_0 = 0.095 \times 10^6$ s^{-1} and $\alpha = 0.87$, for fresh and 3-day old solutions, respectively (cf. Figure 5). These results fit the interpretation that MV^{2+} reduction involves trapped electrons. It can be expected that not all trapping sites are equally accessible to acceptor molecules, so that there will be a distribution in rate constants. Aging will give dye molecules a chance to find optimum binding sites and may reduce the heterogeneity of electron-trapping sites at the particle surface. This interpretation also accounts for the time profile of MV^+ signal growth in the MV^{2+}/TiO_2 sample. In this system, signal growth can be described by a first-order exponential with a time independent rate constant ($k_0 = 0.41 \times 10^6$ s^{-1}). This points to a homogeneous distribution of trapping sites in the TiO_2 particles that becomes heterogeneous upon dye adsorption.

In the case of C343/MV^{2+}/TiO_2, photodegradation of the samples is very slow, showing that the electron-transfer process is nearly fully reversible. MV^+ signal decay, therefore, reflects a back electron-transfer process. It is noteworthy that the decays can be fit quite well (cf. Figures 4 and 5) with a single exponential with a rate which increases as the free radical yield increases. For instance, as illustrated in Figure 5, aging more than doubles the MV^+ yield. At the same time, a least-squares analysis of the time profiles of signal intensities reveals that the rate of decay increases from 1.3×10^2 s^{-1} to 3.8×10^2 s^{-1} upon aging. The radical concentration dependence is explained as follows. Back electron transfer involves collisional encounters of MV^+ with TiO_2 particles. Only encounters that bring MV^+ and $C343^+$ radicals within electron-transfer range will be effective so that a back reaction cross section can be associated with the particles that varies with $C343^+$ coverage. Under the conditions of the experiments the particle concentration is $\sim 10^{-5}$ M. Since upon completion of the forward reaction the MV^+ concentration is in the 10^{-4} to 10^{-3} M range, a particle may hold 10 or more $C343^+$ molecules. With increasing yield of forward electron transfer, the number of $C343^+$ per TiO_2 particle increases, giving rise to an increased back electron-transfer rate.

A final point to be discussed in connection with the EPR spectra displayed in Figure 1 concerns the observed difference in line widths. The spectra of MV^+ in C343/MV^{2+}/ethanol and C343/MV^{2+}/TiO_2 (cf. Figure 1a,c) show well-resolved hyperfine structure, while in MV^{2+}/TiO_2 the structure is partially wiped out due to line broadening (cf. Figure 1b). The broadening is attributed to a high local radical concentration in the MV^{2+}/TiO_2 system. Since the TiO_2 particle concentration is $\sim 10^{-5}$ M and the MV^+ concentration is estimated to be $\sim 10^{-4}$ M, the laser pulse generates ~10 free radicals at the particle surface. The fact that the radicals are born in close vicinity can lead to line broadening due to spin−spin interactions. This effect may be exacerbated by the tendency of bipyridinium cation radicals to form dimers.[32] In the other two systems, the free radicals are distributed homogeneously (in the C343/MV^{2+}/TiO_2 system because of the low reaction rate) so that line-broadening effects are minimized.

IV. Conclusions

The study shows that FT-EPR can be a valuable source of information on the mechanism and kinetics of photoinduced electron-transfer reactions in colloidal TiO_2 solutions. Because of the high spectral resolution, free radicals can be identified unequivocally. Kinetic data can be extracted readily from time profiles of intensities of resonance peaks. The technique may be of particular value in studies of systems, such as a semiconductor film in contact with liquid solution, where light scattering precludes time-resolved optical absorption measurements.

The observation that in the C343/MV^{2+}/TiO_2 system the rate of electron transfer from semiconductor particle to acceptor in solution is strongly attenuated as the coverage approaches saturation level is of particular interest. It provides direct experimental support for the suggestion[33] that the efficiency of the photovoltaic cell designed by Grätzel and co-workers depends in part on the degree of coverage of the nanocrystalline TiO_2 photoanode, by an insulating layer which inhibits direct return of electrons injected into the conduction band to I_3^- present in solution. The effect will play an important role in all redox processes catalyzed by large bandgap semiconductors of which the photoresponse is extended into the visible by adsorption of dye molecules.

References and Notes

(1) Pichat, P.; Fox, M. A. In *Photoinduced Electron Transfer*; Fox, M. A., Chanon, M., Eds.; Elsevier: Amsterdam, 1988; Part D-6.

(2) (a) Kalyanasundaram, K. In *Energy Resource through Photochemistry and Catalysis*; Grätzel, M., Ed.; Academic Press: New York, 1983; Chapter 7. (b) Matheus, R. W. In *Photochemical Conversion and Storage of Solar Energy*; Pelizzetti, E., Schiavello, M., Eds.; Kluwer Academic Publishers: Dordrecht, 1991; p 427.

(3) Mills, A.; Davies, R. H.; Worsley, D. *Chem. Soc. Rev.* **1993**, 417.

(4) Howe, R. F.; Grätzel, M. *J. Phys. Chem.* **1985,** *89*, 4495.

(5) Micic, O. I.; Zhang, Y.; Cromack, K. R.; Trifunac, A. D.; Thurnauer, M. C. *J. Phys. Chem.* **1993**, *97*, 7277.

(6) Micic, O. I.; Zhang, Y.; Cromack, K. R.; Trifunac, A. D.; Thurnauer, M. C. *J. Phys. Chem.* **1993**, *97*, 13284.

(7) Rajh, T.; Ostafin, A. E.; Micic, O. I.; Tiede, D. M.; Thurnauer, M. C. *J. Phys. Chem.* **1996**, *100*, 4538.

(8) Noda, H.; Oikawa, K.; Ohya-Nishiguchi, H.; Kamada, H. *Bull. Chem. Soc. Jpn.* **1993**, *66*, 3542.

(9) Noda, H.; Oikawa, K.; Kamada, H. *Bull. Chem. Soc. Jpn*. **1993**, *66*, 455.

(10) Kaise, M.; Kondoh, H.; Nishihara, C.; Nozoye, H.; Shindo, H.; Nimura, S.; Kikuchi, O. *J. Chem. Soc., Chem. Commun.* **1993**, 395.

(11) Kaise, M.; Nagai, H.; Tokuhashi, K.; Kondo, S.; Nimura, S.; Kikuchi, O. *Langmuir* **1994**, *10*, 1345.

(12) Bowman, M. K. In *Modern Pulsed and Continuous-Wave Electron Spin Resonance*; Kevan, L., Bowman, M. K., Eds.; Wiley: New York, 1990, Chapter 1.

(13) Enea, O.; Moser, J.; Grätzel, M. *J. Electroanal. Chem.* **1989**, *259*, 59.

(14) Moser, J.; Grätzel, M. *J. Am. Chem. Soc*. **1984**, *106*, 6557.

(15) De Silvestro, J.; Grätzel, M.; Kavan, L.; Moser, J.; Augustynski, J. *J. Am. Chem. Soc*. **1985**, *107*, 2988.

(16) Kalyanasundaram, K.; Vlachpoulos, N.; Krishnan, V.; Monnier, A.; Grätzel, M. *J. Phys. Chem*. **1987**, *91*, 2342.

(17) Kamat, P. V. *Inter-Am. Photochem. Soc. Newslett.* **1960**, *19*, 14.

(18) Kamat, P. V.; Bedja, I.; Hotchandani, S. *J. Phys. Chem*. **1994**, *98*, 9137.

(19) van Willigen, H.; Levstein, P. R.; Ebersole, M. H. *Chem. Rev.* **1993**, *93*, 173.

(20) Levstein, P. R.; van Willigen, H. *J. Chem. Phys.* **1991**, *95*, 900.

(21) de Beer, R.; van Ormondt, D. In *Advanced EPR: Applications in Biology and Biochemistry*; Hoff, A. J., Ed.; Elsevier: Amsterdam, 1989; p 135.

(22) Rieger, A. L.; Rieger, P. H. *J. Phys. Chem*. **1984**, *88*, 5845.

(23) McLauchlan, K. A. In *Modern Pulsed and Continuous-Wave Electron Spin Resonance*; Kevan, L., Bowman M. K., Eds.; Wiley: New York, 1990; Chapter 7.

(24) Duonghong, D.; Ramsden, J.; Grätzel, M. *J. Am. Chem. Soc*. **1982**, *104*, 2977.

(25) Fox, M. A.; Lindig, B.; Chen, C. S. *J. Am. Chem. Soc*. **1982**, *104*, 5828.

(26) Yan, S. G.; Hupp, J. T. *J. Phys. Chem*. **1996**, *100*, 6867.

(27) See for example: (a) Bolts, J. M.; Wrighton, M. S. *J. Phys. Chem*. **1976**, *80*, 2641. (b) Gerisher, N. *Electrochim. Acta* **1989**, *34*, 1005.

(28) Rehm, J. M.; McLendon, G. L.; Nagasawa, Y.; Yoshihara, K.; Moser, J.; Grätzel, M. *J. Phys. Chem*. **1996**, *100*, 9577.

(29) Iwasaki, T.; Oda, S.; Sawada, T.; Honda, K. *J. Phys. Chem.* **1980**, *84*, 2800.

(30) For the C343/MV^{2+}/TiO_2 solution measured after a 3-day aging period, the FID was the time average of signals generated by only 120 laser shots (30/phase).

(31) (a) Palmer, R. G.; Stein, D. L.; Abrahams, E.; Anderson, P. W. *Phys. Rev. Lett.* **1984**, *53*, 958. (b) Ford, W. E.; Rodgers, M. A. J. *J. Phys. Chem.* **1994**, *98*, 3822.

(32) (a) Evans, A. G.; Evans, J. C.; Baker, M. W. *J. Chem. Soc., Perkin Trans. 2* **1977**, 1787. (b) Evans, A. G.; Evans, J. C.; Baker, M. W. *J. Am. Chem. Soc*. **1977**, *99*, 5882.

(33) Nazeeruddin, M. K.; Kay, A.; Rodicio, I.; Humphry-Baker, R.; Müller, E.; Liska, P.; Vlachopoulos, N.; Grätzel, M. *J. Am. Chem. Soc.* **1993**, *115*, 6382.